Isomerization and Dissociation of CHNS: Quantum Mechanical Study

2 AUTHORS, INCLUDING:

Maria Wierzejewska
University of Wroclaw
61 PUBLICATIONS **475** CITATIONS

Isomerization and Dissociation of CHNS: Quantum Mechanical Study

Maria Wierzejewska* and Jerzy Moc

Faculty of Chemistry, University of Wrocław, F. Joliot-Curie 14, 50-383 Wrocław, Poland

Received: August 15, 2003; In Final Form: October 16, 2003

An extensive quantum mechanical study of the potential energy surface for the isomerization and dissociation reactions of CHNS is reported. The calculations were performed using density functional theory and correlated ab initio methods and employing large aug-cc-pVTZ basis set. Nine CHNS isomers and eleven transition states linking them have been found on the singlet PES. Dissociation energies of the singlet most stable open chain CHNS isomers have been evaluated. On the triplet PES, eight mostly highly energetic CHNS isomers and five transition states for their interconversion and dissociation have been also found. Several available routes for isomerization and dissociation have been identified. A prediction has been made for the possible mechanism explaining the formation of the singlet HSCN and HSNC during UV photolysis of HNCS/Ar and HNCS/N_2 low-temperature matrixes observed recently by one of us.

1. Introduction

Although the isothiocyanic acid HNCS has been known for many years and is now relatively well described,[1−9] not much information is available on the other isomers of the general formula CHNS. Very recently, it was shown in our laboratory[10] by means of FTIR matrix isolation spectroscopy that UV photolysis of the isothiocyanic acid HNCS led to the formation of two new isomers: thiocyanic acid HSCN and isothiofulminic acid HSNC. The mechanism of the HNCS photoisomerization observed in the low-temperature matrixes is of considerable interest. On the basis of the experimental findings alone, it was not possible to draw definite conclusions concerning the pathways of the HSCN and HSNC formation.[10] Moreover, the available theoretical data for the CHNS isomers are far from complete and have been mostly obtained at the low level of theory while those dealing with structure and energetics of the possible isomerization transition states are not existent at all.

In this paper, we present results of an extensive quantum chemical study on the singlet and triplet potential energy surface (PES) of CHNS carried out to determine possible isomeric structures of this species, the related isomerization pathways, and to provide reliable energetics. Dissociation processes of the low-energy isomers have been studied as well. Also, one of the aims of this work is to indicate among the calculated isomerization and dissociation reactions those which might have occurred under the reported experimental conditions[10] and thus help to suggest the likely mechanism of the photolytic reaction which has taken place in the HNCS/Ar and HNCS/N_2 matrixes.

2. Computational Methods

The all-electron augmented correlation-consistent polarized valence triple-ζ (aug-cc-pVTZ) basis set was used throughout.[11−13] At first, calculations were carried out with density functional theory (DFT) using B3LYP functional.[14,15] Structures of the CHNS isomers and isomerization transition states were found along with the associated force constant matrixes calculated to characterize the stationary points and to evaluate harmonic frequencies and zero-point vibrational energy (ZPE) corrections.

* Corresponding author. E-mail address: mw@wchuwr.chem.uni.wroc.pl.

Spin-restricted and spin-unrestricted calculations were carried out for singlets and triplets, respectively. For reaction paths, minima were connected to each transition state (TS) by following intrinsic reaction coordinate (IRC)[16,17] generated at the B3LYP level. Next, structures of all the singlet minima found as well as those of the singlet transition states involved in the paths of the experimental relevance were recalculated with ab initio second-order Møller−Plesset perturbation theory (MP2)[18] within the frozen-core approximation. The energetics of the MP2 structures were improved by single-point calculations with ab initio coupled-cluster singles and doubles method including a perturbative estimate of triples (CCSD(T)).[19] The CCSD(T)// MP2 relative energies were corrected for the MP2 ZPE values. The B3LYP//B3LYP and CCSD(T)//MP2 relative energies discussed below have the ZPE corrections included. All calculations were performed using Gaussian 98 code.[20]

3. Results and Discussion

3.1. Singlet and Triplet CHNS Isomers. Although the isothiocyanic acid HNCS and three other open-chain CHNS isomers have been studied earlier at different computational levels,[5,6,21−23] no systematic theoretical study of the CHNS isomers has been reported. The available results point to the isothiocyanic acid HNCS as the most stable isomer and the thiocyanic acid HSCN as the second most stable. The remaining two isomers containing the CNS unit, thiofulminic HCNS and isothiofulminic HSNC acids, have been calculated to be the third and fourth most stable.

The present calculations have revealed nine minima on the singlet CHNS potential energy surface and eight minima on the triplet PES as shown in Figures 1 and 2, respectively, with the associated energetics included in Table 1. Among the nine minima found on the singlet PES, six correspond to the open-chain structures and three to cyclic structures. Their relative B3LYP//B3LYP energies increase in the following order: HNCS(0.0 kcal/mol) < HSCN(11.8) < HCNS(34.3) < HSNC(40.3) < cyclic-C(H)NS(50.8) < cyclic-S(H)CN(59.3) < cyclic-N(H)CS(76.4) < HNSC(127.0) < HCSN(127.6). The corresponding energies obtained from the CCSD(T)//MP2 calculation are HNCS(0.0 kcal/mol) < HSCN(6.3) < HCNS(34.4) < HSNC(36.0) < cyclic-C(H)NS(45.0) < cyclic-S(H)CN(54.2) <

TABLE 1: Relative Energies ($\Delta E + \Delta ZPE$) of Various Singlet and Triplet CHNS Isomers and Isomerization and Dissociation Transition States (in kcal/mol)

isomer[a]		B3LYP//B3LYP	CCSD(T)//MP2	transition state[a]		B3LYP//B3LYP	CCSD(T)//MP2
HNCS (C_s)		0.0	0.0	TS0 ($C_{\infty v}$)		1.6	1.9
HSCN (C_s)		11.8	6.3	TS1 (C_s)		62.4	60.3
HCNS (C_v)		34.3	34.4	TS2 (C_s)		94.1	92.6
HSNC (C_s)		40.3	36.0	TS3 (C_1)		59.5	54.3
cyclic-C(H)NS (C_s)		50.8	45.0	TS4 (C_1)		63.0	58.0
cyclic-S(H)CN (C_1)		59.3	54.2	TS5 (C_1)		86.0	
cyclic-N(H)CS (C_s)		76.4	72.1	TS6 (C_1)		108.1	
HNSC (C_s)		127.0	120.6	TS7 (C_1)		77.6	
HCSN (C_s)		127.6	125.1	TS8 (C_s)		95.0	
branched-C(H) NS (C_s)	³A″	62.6		TS9 (C_s)		91.9	
HNCS (C_1)	³A	67.1		TS10 (C_s)		83.4	
HCNS (C_s)	³A′	79.9					
cyclic-C(H)NS (C_1)	³A	90.0		TS1t (C_1)	³A	102.5	
HSCN(C_1)	³A	90.1		TS2t (C_s)	³A′	126.1	
HSNC (C_1)	³A	100.0		TS3t (C_1)	³A	103.9	
HNSC(C_s)	³A″	126.9		TS4t (C_s)	³A″	72.6	
HCSN(C_1)	³A	127.2		TS5t (C_s)	³A″	100.7	

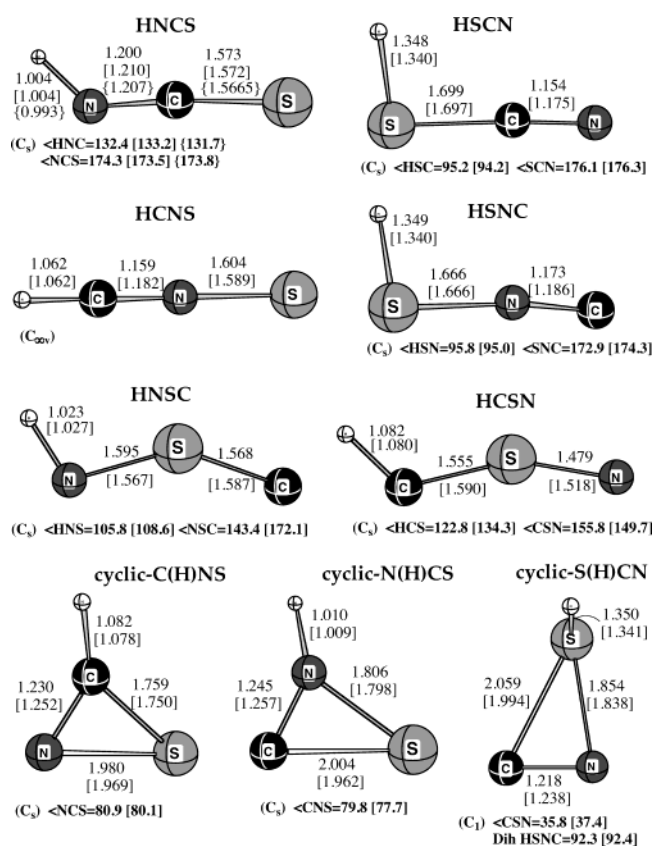[a] If not indicated, the electronic state of the species is a closed-shell singlet.

Figure 1. Minima found on the singlet CHNS potential energy surface using B3LYP and MP2 methods. Bond lengths are in Å, bond angles and dihedral angles are in degrees; numbers in square brackets are from MP2 calculations, whereas those in curly brackets are from experiment.[2]
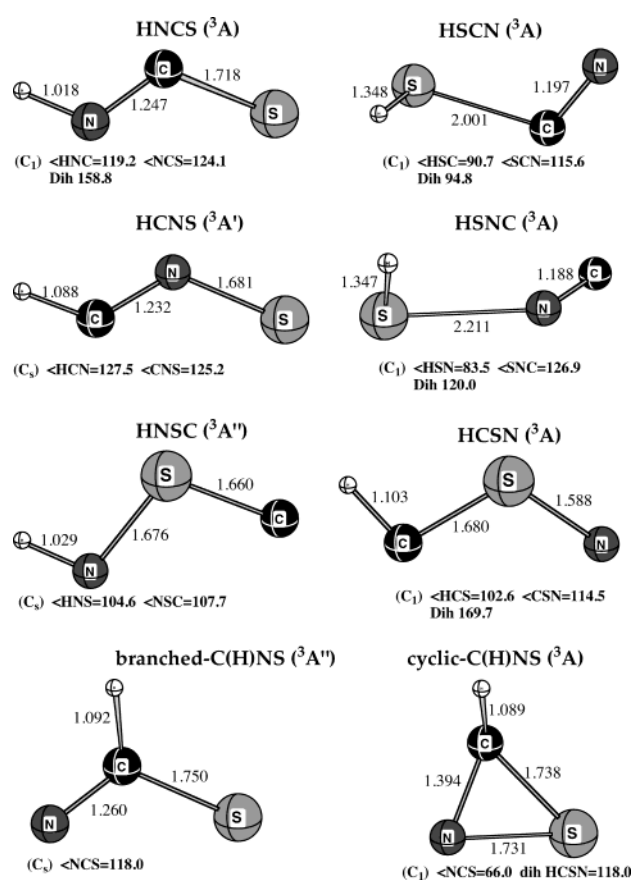

Figure 2. Minima found on the triplet CHNS potential energy surface using B3LYP method. Bond lengths are in Å, bond angles and dihedral angles are in degrees.

cyclic-N(H)CS(72.1) < HNSC(120.6) < HCSN(125.1). It is clear from this comparison that the stability order is the same at both levels of theory and that the dynamic correlation explicit in CCSD(T) extrastabilize most isomers, usually by ca. 4−5 kcal/mol relative to the B3LYP results. The last two open-chain isomers containing the CSN unit have not been studied so far and the same holds true for the three cyclic structures. As HNSC and HCSN lie significantly higher in energy as compared to the remaining singlet isomers, possible rearrangements involving the two species have not been studied here. The cyclic-C(H)-NS and cyclic-N(H)CS are planar (C_s) while the cyclic-S(H)-CN has C_1 symmetry with the HSNC dihedral angle of 92.3(92.4°) at the B3LYP(MP2) level.

As can be seen from Figure 2, among the eight triplet CHNS isomers found, six are the open-chain species, whose structures deviate appreciably from the singlet analogues. The triplet counterparts of cyclic-N(H)CS and cyclic-S(H)CN have not been located; the starting cyclic structures always optimized to the open-chain forms. The only genuine cyclic triplet isomer is the cyclic-C(H)NS (³A) of no symmetry with the HCSN dihedral angle of 118°. The last triplet structure, termed branched-C(H)-NS (³A″), is planar. It lacks the N−S bond, with the N···S distance of 2.59 Å. This species appeared to be the most stable triplet isomer. The calculated B3LYP//B3LYP stability order of the triplet isomers is the following: branched-C(H)NS(³A″)-(62.6kcal/mol) < HNCS(³A)(67.1) < HCNS(³A′)(79.9) <

Isomerization and Dissociation of CHNS

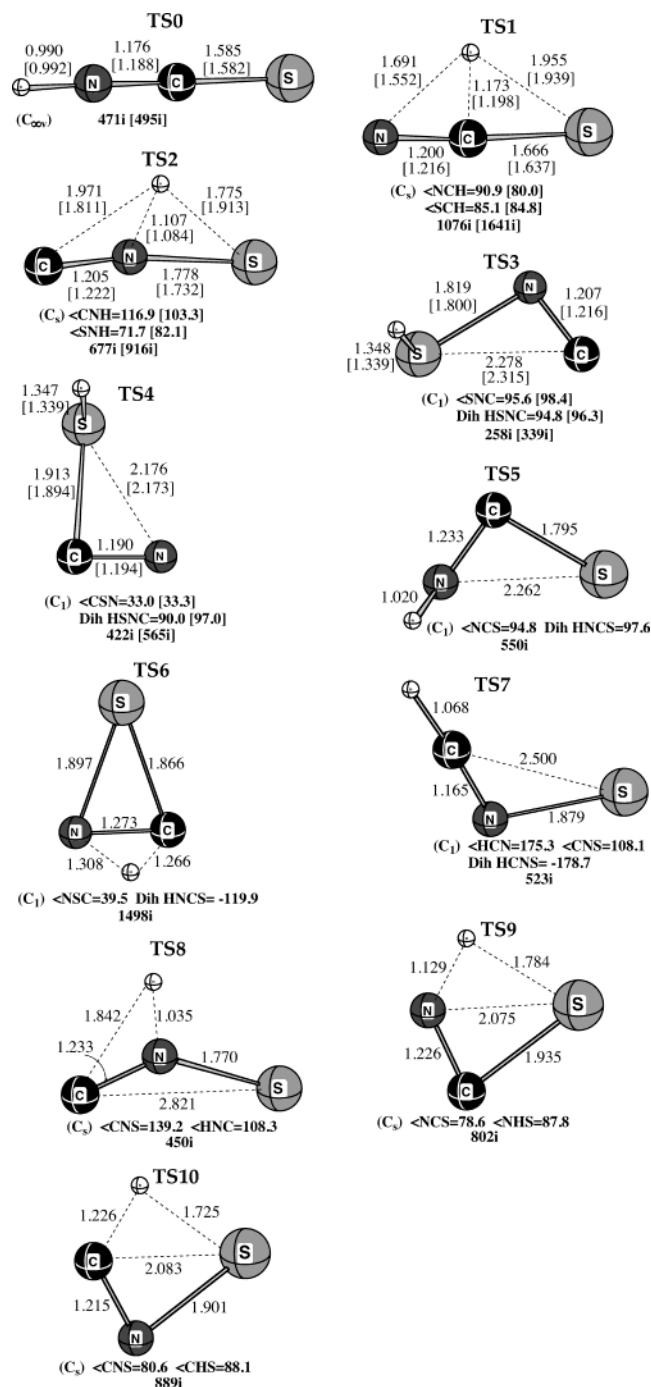*J. Phys. Chem. A, Vol. 107, No. 50, 2003* **11211**

Figure 3. Isomerization transition states on singlet CHNS potential energy surface calculated using B3LYP and MP2 methods. Bond lengths are in Å, bond angles and dihedral angles are in degrees; the magnitudes of imaginary frequencies (in cm^{-1}) are included. Numbers in square brackets are from MP2 calculations.

Figure 4. Overview of the isomerization pathways for singlet CHNS. Relative energies in bold refer to the minima and those in italics refer to the transition states linking them. All values (kcal/mol) have been obtained at the ZPE corrected B3LYP//B3LYP level.

3.2. Isomerization Pathways for the Singlet CHNS Species. The located transition states connecting the singlet CHNS isomeric structures are displayed in Figure 3 with an overview indicating isomerization pathways shown in Figure 4. The associated energetics is included in Table 1. The activation barriers for all the singlet isomerization reactions considered, both forward and backward, are summarized in Table 2, while Figure 5 illustrates the related potential energy diagram. Note that for consistency only the B3LYP//B3LYP energies are given in Figures 4 and 5. The available CCSD(T)// MP2 energies are included for comparison in Tables 1 and 2.

HNCS ↔ HNCS. As already mentioned and in agreement with the results of previous calculations,[21−23] the most stable isomer is HNCS of C_s symmetry; it assumes the trans bent conformation with NCS and HNC angles of 174.3/173.5° and 132.4/ 133.2°, respectively. Our computed structures of HNCS are in excellent agreement with experiment.[2] A degenerate HNCS ↔ HNCS rearrangement proceeds through the linear TS0 transition state (Figure 3) with the energetic barrier to linearity as low as 1.6/ 1.9 kcal/mol. As seen from Figures 1 and 3, TS0 shows slightly shortened HN and NC bonds and lengthened CS distance as compared to HNCS.

HNCS → HSCN and HCNS → HSNC. There are two concerted isomerizations possible between the open-chain species. The first one is a rearrangement of HNCS to HSCN that occurs by a direct 1,3-hydrogen transfer, from N to S, through the TS1 transition state. The TS1 is planar with the a′ imaginary frequency of 1076i/1641i cm^{-1} and the NCH angle of 90.9/80.0° (Figure 3). The HSCN product is the second most stable isomer lying 11.8/6.3 kcal/mol higher than HNCS. The barrier height for the HNCS → HSCN reaction is 62.4/60.3 kcal/ mol and that for the reverse process is calculated as 50.6/54.0 kcal/mol (Table 2).

The third most stable isomer, HCNS, may rearrange to HSNC also by a direct 1,3 hydrogen shift from C to S through TS2. The transition state involved is again planar with the hydrogen tilted toward S atom, the SNH angle being 71.7/82.1°. Despite the fact that TS2 is placed as high as 94.1/92.6 kcal/mol above the global minimum, the activation energy for the HCNS → HSNC reaction of 59.8/58.2 kcal/mol is similar to that predicted for the HNCS → HSCN isomerization via TS1. The former process is predicted to be endothermic by 6.0/1.6 kcal/mol (Figure 5).

HSNC → cyclic-S(H)CN and HSCN → cyclic-S(H)CN. Both open structures HSNC and HSCN can rearrange endothermically

cyclic-C(H)NS(^{3}A)(90.0) < HSCN(^{3}A)(90.1) < HSNC(^{3}A)-(100.0) < HNSC(^{3}A″)(126.9) < HCSN(^{3}A) (127.2), where the energies in parentheses are relative to the singlet HNCS global minimum. The calculated relative energies for the triplet CHNS isomers reveal that even the most stable triplet species, branched-C(H)NS(^{3}A″) lying ca. 63 kcal/mol above the singlet global minimum, is clearly higher in energy than the six most stable singlet species (cf. Table 1).

From now on the structures and energetics discussed in sections 3.2, 3.3, and 3.4 are those from the B3LYP calculations. The available MP2 geometrical parameters or the CCSD(T)// MP2 energies are given after slash.
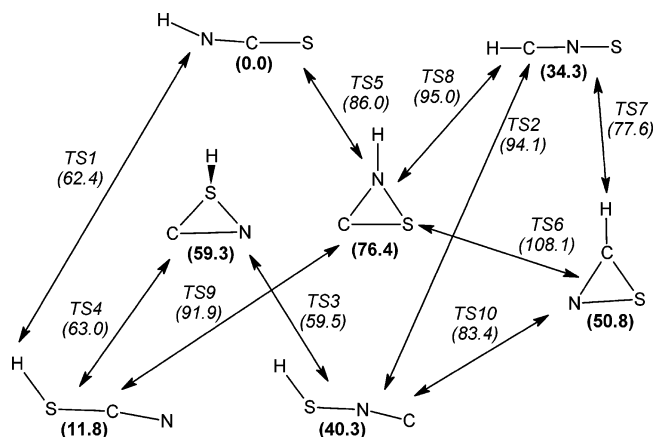
TABLE 2: Energy Barriers (in kcal/mol) for the Isomerization Reactions of Singlet CHNS Species Calculated at the ZPE Corrected B3LYP//B3LYP Level

reaction	energy barrier[a]	reaction	energy barrier[a]
HNCS → HSCN	62.4/60.3	HSCN → HNCS	50.6/54.0
HCNS → HSNC	59.8/58.2	HSNC → HCNS	53.8/56.6
HSNC → cyclic-S(H)CN	19.2/18.3	cyclic-S(H)CN → HSNC	0.2/0.1
HSCN → cyclic-S(H)CN	51.2/51.7	cyclic-S(H)CN → HSCN	3.7/3.8
HNCS → cyclic-N(H)CS	86.0	cyclic-N(H)CS → HNCS	9.6
cyclic-N(H)CS → cyclic-C(H)NS	31.7	cyclic-C(H)NS → cyclic-N(H)CS	57.3
cyclic-C(H)NS → HCNS	26.8	HCNS → cyclic-C(H)NS	43.3
cyclic-N(H)CS → HCNS	18.6	HCNS → cyclic-N(H)CS	60.7
cyclic-N(H)CS → HSCN	15.5	HSCN → cyclic-N(H)CS	80.1
cyclic-C(H)NS → HSNC	32.6	HSNC → cyclic-C(H)NS	43.1

[a] The values after slash are the ZPE corrected CCSD(T)//MP2 ones.
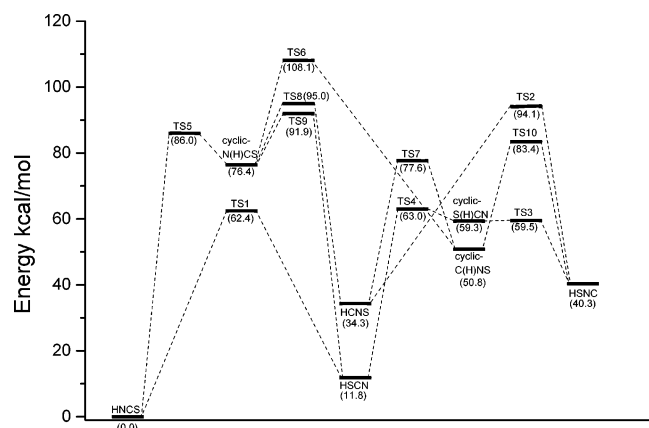
Figure 5. ZPE corrected B3LYP//B3LYP potential energy diagram for isomerization of singlet CHNS.

to form the cyclic-S(H)CN via TS3 and TS4, respectively (Figures 4 and 5). The two processes ending up with a ring closing proceed through the productlike transition states of C_1 symmetry featuring hydrogen atom perpendicular to the SCN plane. Although TS3 and TS4 are comparable in energy, lying 59.5/54.3 and 63.0/58.0 kcal/mol above HNCS, the HSNC → cyclic-S(H)CN reaction via TS3 requires much less activation energy (19.2/18.3 kcal/mol) relative to that required to traverse from HSCN to cyclic-S(H)CN through TS4 (51.2/51.7 kcal/mol). This is due to the significant difference in stability between the two open-chain species. The cyclic-S(H)CN resides in a very shallow potential well with the barriers separating it from HSNC and HSCN of 0.2/0.1 and 3.7/3.8 kcal/mol, respectively (cf. Figure 5, Table 2). These low barriers do not ensure kinetic stability of the cyclic-S(H)CN species in the gas phase. It is obvious from these results that the HSCN → HSNC isomerization can be accomplished via a two-step mechanism with the cyclic-S(H)CN as intermediate. Overall, this reaction is endothermic by 28.5/29.7 kcal/mol with the higher barrier to overcome, via TS4, being 51.2/51.7 kcal/mol relative to HSCN.

HNCS → cyclic-N(H)CS → cyclic-C(H)NS. The lowest energy isomer HNCS rearranges endothermically to the cyclic-N(H)-CS via TS5. The endothermicity of this step is significant, 76.4/72.1 kcal/mol. The TS5 has C_1 symmetry with the nearly formed CNS cycle and the H atom positioned almost perpendicularly to the NCS plane. The reaction coordinate involves the NCS angle decrease leading to the N−S bond formation and a ring closure. The resultant cyclic-N(H)CS has the highest energy of all the singlet CHNS species for which the isomerizations are considered. Accordingly, an appreciable energy barrier for the forward reaction proceeding via TS5 of 86.0 kcal/mol is predicted. The barrier for the reverse process is only 9.6 kcal/mol (Figure 5, Table 2).

As Figure 5 shows, the cyclic-N(H)CS can izomerize further via three exothermic channels involving high-energy transition states. The highest of them leads to another cyclic structure C(H)NS. The reaction occurs through the hydrogen shift and involves the cyclic TS6 lying at 108.1 kcal/mol. At this transition state, the H atom takes the intermediate position between the N and C atoms and as the reaction coordinate is followed, the H−N bond is eventually broken and the cyclic-C(H)NS is formed. The latter species is the most stable among the three cyclic singletisomers, lying 50.8/45.0 kcal/mol above the global minimum. TS6 is the highest energy point on the singlet CHNS isomerization PES in Figure 5 with the energy barrier for the cyclic-N(H)CS → cyclic-C(H)NS isomerization 31.7 kcal/mol.

Cyclic-N(H)CS → HCNS and cyclic-N(H)CS → HSCN. Alternatively, the cyclic-N(H)CS can rearrange to HCNS in the exothermic step (by 42.1 kcal/mol) through the TS8 transition state placed at 95.0 kcal/mol (Figure 5). This process is accompanied by the H transfer from N to C and the ring opening which destroys the C−S bond. TS8 is planar and features the CNS angle of 139.2° and essentially broken C−S bond with the C−S distance of 2.82 Å (Figure 3).

The cyclic-N(H)CS can also convert into very stable HSCN via the ringlike TS9 lying 91.9 kcal/mol above HNCS. This process involving the hydrogen shift and ring opening is exothermic by 64.6/65.8 kcal/mol. The corresponding energy barrier for the HSCN formation with respect to the cyclic-N(H)-CS is 15.5 kcal/mol.

Cyclic-C(H)NS → HCNS and cyclic-C(H)NS → HSNC. The opening of cyclic-C(H)NS to HCNS proceeds via TS7. The process is exothermic by 16.5/10.6 kcal/mol. The transition state features the CNS angle of 108.1° and the nearly broken (2.5 Å) C−S bond while the HCN unit is almost linear as in the product. The energy of TS7 with respect to the global minimum is 77.6 kcal/mol, but the activation energy for the cyclic C(H)-NS → HCNS interconversion is fairly low and equals 26.8 kcal/mol.

Another way of converting the cyclic-C(H)NS isomer into more stable HSNC open isomer is through the ringlike TS10 transition state lying 83.4 kcal/mol higher than HNCS. This rearrangement involves again the hydrogen shift and ring opening and is exothermic by 10.5/9.0 kcal/mol. The calculated energy barrier for the HSNC formation with respect to the cyclic-C(H)NS is 32.6 kcal/mol.

3.3. Dissociation Limits of the Singlet CHNS Isomers. Selected dissociation pathways of five open-chain singlet CHNS isomers have been investigated. The obtained values of the dissociation energies are summarized in Table 3 together with the available experimental data while Figure 6 shows the related energy diagram. The dissociation products are calculated in their ground electronic state. Among the reactions included, those yielding the triplet fragments are spin forbidden. As can be seen

Isomerization and Dissociation of CHNS

J. Phys. Chem. A, Vol. 107, No. 50, 2003 **11213**

TABLE 3: Relative Energies ($\Delta E + \Delta$ZPE) of the Dissociation Products of the Various Open-Chain Singlet CHNS Isomers (in kcal/mol)[c]

	energy of the products		
reaction	B3LYP//B3LYP	CCSD(T)//MP2	experiment[a]
HNCS → HNC($^1\Sigma^+$) + S(^{3}P)	80.5	74.7	80.6
HNCS → H(^{2}S) + NCS($^2\Pi$)	89.0	89.6	97.1
HNCS → NH($^3\Sigma^-$) + CS($^1\Sigma^+$)	123.6	115.6	120.2
HSCN → H(^{2}S) + NCS($^2\Pi$)	89.0	89.6	97.1
HSCN → SH($^2\Pi$) + CN($^2\Sigma^+$)	110.0	108.5	108.6 (100.3[b])
HSNC → SH($^2\Pi$) + CN($^2\Sigma^+$)	110.0	108.5	108.6 (100.3[b])
HSNC → H(^{2}S) + CNS($^2\Pi$)	117.5	115.9	
HCNS → HCN($^1\Sigma^+$) + S(^{3}P)	67.0	60.1	65.6
HCNS → H(^{2}S) + CNS($^2\Pi$)	117.5	115.9	
HNSC → NH($^3\Sigma^-$) + CS($^1\Sigma^+$)	123.6	115.6	120.2

[a] Values estimated from data.[9] [b] Value from laser-induced fluorescence experiment.[28] [c] The products are in their ground electronic state.
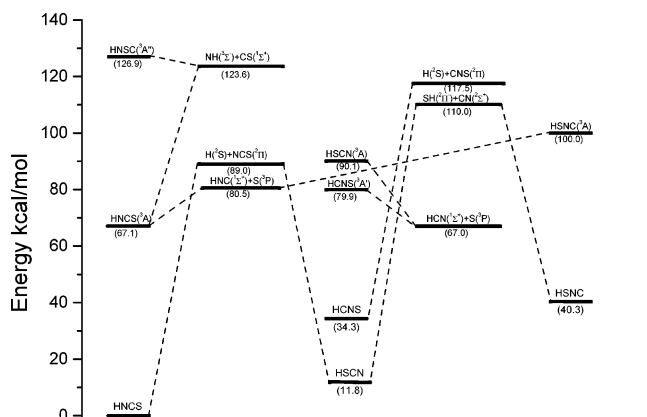

Figure 6. ZPE corrected B3LYP//B3LYP energy level diagram of CHNS including dissociation limits. The dissociation products are in their ground electronic state. Note that the barriers to dissociation have not been systematically studied (cf. also Figure 9).

from Table 3, the calculated dissociation energies are in accord with the ΔH_0 values estimated on the basis of the photoionization mass spectrometric studies performed by Russic and Berkovitz[9] for the corresponding processes. In general, there is also a good agreement between the calculated DFT and ab initio values. According to Table 3, the HNC($^1\Sigma^+$) + S(^{3}P), H(^{2}S) + NCS($^2\Pi$), NH($^3\Sigma^-$) + CS($^1\Sigma^+$) dissociation fragments lie 80.5/74.7, 89.0/89.6, 123.6/115.6 kcal/mol, respectively, above the singlet HNCS. The experimental estimates are 80.6, 97.1, and 120.2 kcal/mol, respectively.

3.4. Isomerization and Dissociation Pathways for the Triplet CHNS Species. Five transition states located on the triplet CHNS potential energy surface, two of them being dissociative transition states, are presented in Figure 7 with their energetics included in Table 1. The related activation barriers for the considered isomerization and dissociation reactions are given in Table 4. An overview indicating isomerization and dissociation pathways and the corresponding triplet potential energy diagram are shown in Figures 8 and 9, respectively.

Branched-C(H)NS(^{3}A″) → HNCS(^{3}A), Branched-C(H)NS(^{3}A″) → HSCN(^{3}A). The branched-C(H)NS(^{3}A″) and HNCS(^{3}A) represent two most stable triplet species, with the energies relative to the global minimum of 62.6 and 67.1 kcal/mol, respectively. The two triplet isomers interconvert through one step mechanism. The reaction is a 1,2-hydrogen shift from C to N occurring through the TS1t(^{3}A) transition state (Figure 7) located at 102.5 kcal/mol with respect to the global minimum (Figure 9). TS1t(^{3}A) shows a cyclic structure of C_1 symmetry in which the N, C, and H atoms form a triangle and the sulfur atom is positioned out of the plane with the SCNH dihedral angle of 137.4°.
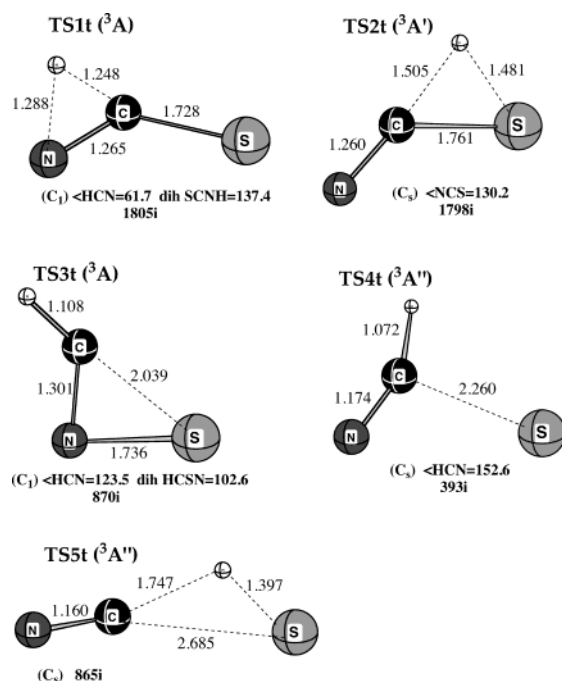

Figure 7. Isomerization and dissociation transition states on the triplet CHNS potential energy surface calculated using B3LYP method. Bond lengths are in Å, bond angles and dihedral angles are in degrees; the magnitudes of imaginary frequencies (in cm^{-1}) are included.

The branched-C(H)NS(^{3}A″) species can also rearrange through a 1,2-hydrogen shift from C to S leading to HSCN(^{3}A). The process involves a high-energy planar TS2t(^{3}A″) transition state placed at 126.1 kcal/mol above the singlet HNCS.

Both branched-C(H)NS(^{3}A″) → HNCS(^{3}A) and branched-C(H)NS(^{3}A″) → HSCN(^{3}A) channels are endothermic by 4.5 and 27.5 kcal/mol, respectively.

HCNS(^{3}A′) → cyclic-C(H)NS(^{3}A). The HCNS(^{3}A′) is calculated to be the third most stable triplet CHNS isomer. We have found that it can rearrange to the cyclic-C(H)NS(^{3}A) species. This interconversion occurs through the transition state TS3t-(^{3}A) and the process involves a formation of the C−S bond resulting in the ring structure of the product. The cyclic-C(H)-NS(^{3}A) product having the relative energy of 90 kcal/mol is isoenergetic with the HSCN(^{3}A) triplet isomer and lies ca. 10 kcal/mol above the HCNS(^{3}A′) (Figure 9).

Branched C(H)NS(^{3}A″) → HCN + S(^{3}P) and HSCN(^{3}A) → HCN + S(^{3}P). It appears that the most stable triplet isomer, branched-C(H)NS(^{3}A″) can easily dissociate to the singlet HCN and sulfur atom S(^{3}P). The decomposition proceeds via TS4t(^{3}A″) which is planar with the cleaved C−S bond of 2.26 Å. TS4t-(^{3}A″) is located only 72.6 kcal/mol above the global minimum

TABLE 4: Energy Barriers (in kcal/mol) for the Isomerization and Dissociation Reactions of Triplet CHNS Calculated at the ZPE Corrected B3LYP//B3LYP Level

reaction	energy barrier	reaction	energy barrier
branched-C(H)NS(^{3}A″) → HNCS(^{3}A)	39.9	HNCS(^{3}A) → branched-C(H)NS(^{3}A″)	35.4
branched-C(H)NS(^{3}A″) → HSCN(^{3}A)	63.5	HSCN(^{3}A) → branched-C(H)NS(^{3}A″)	36.0
HCNS(^{3}A′) → cyclic-C(H)NS(^{3}A)	24.0	cyclic-C(H)NS(^{3}A) → HCNS(^{3}A′)	13.9
branched-C(H)NS(^{3}A″) → HCN + S(^{3}P)	10.0	HCN + S(^{3}P) → branched-C(H)NS(^{3}A″)	5.6
HSCN(^{3}A) → HCN + S(^{3}P)	10.6	HCN + S(^{3}P) → HSCN(^{3}A)	33.7
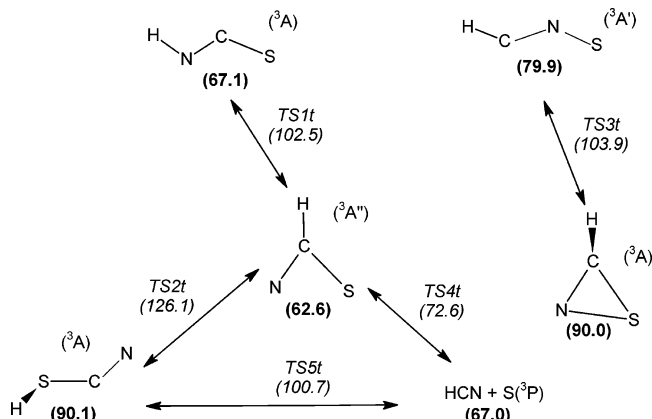
Figure 8. Overview of the isomerization and dissociation pathways for triplet CHNS. Relative energies in bold refer to the minima and those in italics refer to the transition states linking them. All values (kcal/mol) have been obtained at the ZPE corrected B3LYP//B3LYP level.
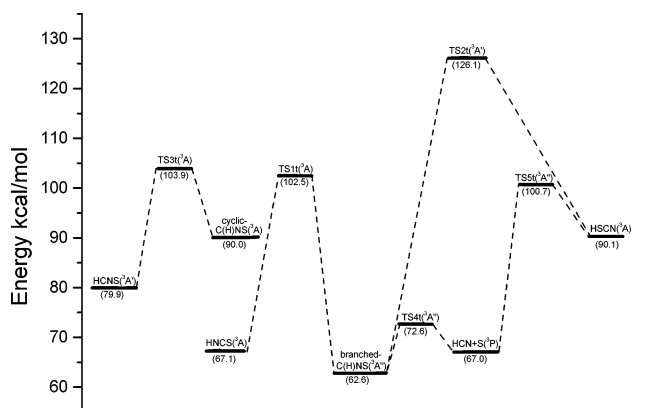
Figure 9. ZPE corrected B3LYP//B3LYP potential energy diagram for isomerization and dissociation of triplet CHNS.

and is the lowest energy transition state found on the triplet PES. The activation energy required for the branched-C(H)-NS(^{3}A″) → HCN + S(^{3}P) dissociation is as low as 10 kcal/mol. The calculated barrier height for the reverse process is only 5.6 kcal/mol (Table 4).

It is possible to obtain the same HCN + S(^{3}P) dissociation products when starting from the triplet HSCN(^{3}A) isomer. Although this reaction is exothermic by 23.1 kcal/mol, it proceeds via a high-energy TS5t(^{3}A″) lying at 100.7 kcal/mol above the global minimum. When the S atom is expelled from HSCN(^{3}A), both the S−H and S−C bonds are broken, but the strong C−H bond is formed instead to yield HCN molecule. The activation barrier for the HSCN(^{3}A) → HCN + S(^{3}P) dissociation of 10.6 kcal/mol is similar to that calculated for the dissociation of the branched-C(H)NS(^{3}A″) (cf. Figure 9).

3.5. The Isomerization of HNCS Species in the Light of the Matrix Infrared Experiment. Recently, it was shown by one of us[10] by using FTIR matrix isolation spectroscopy that HNCS subjected to the UV radiation izomerizes to HSCN and HSNC species. Table 5 presents a comparison between the
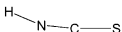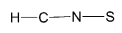
infrared frequencies of the four most stable singlet isomers calculated here at the B3LYP and MP2 levels with those available from the argon matrix experiment.

Several experimental facts are meaningful when considering the possible ways of the isomerization of the singlet HNCS proceeding in the low-temperature matrixes. The first is the observation of two new singlet isomers, HSCN and HSNC, whereas thermodynamically more stable than the latter, singlet HCNS was not detected.[10] Second, both observed HSCN and HSNC species are produced as primary products of the HNCS isomerization. Third, the threshold energy for this photolytic reaction was estimated by using long wavelength pass filters to be 300 nm which corresponds to ca. 95 kcal/mol.[10] Below we consider the likely mechanisms of the photolytic reaction which might help us explain the experimental features observed in the low-temperature matrixes.

3.5.1. Dissociative Mechanism. UV radiation may lead to the dissociation of the initial singlet HNCS molecules and the recombination of the resultant radicals can produce new isomers. Among the three possible dissociation channels considered for the HNCS precursor (see Table 3 and Figure 6), the HNCS → H(^{2}S) + NCS($^2\Pi$) is the only spin-allowed process and a likely candidate for the first step. In fact, the dissociation limit for this process is calculated to be 89.0/89.6 kcal/mol and this value agrees well with the experimental threshold energy of the isomerization process (ca. 95 kcal/mol).[10] The resultant H and NCS radicals may recombine to form either the new isomer HSCN or to reproduce the HNCS species. The singlet HSCN may further dissociate producing the SH($^2\Pi$) and CN($^2\Sigma^+$) radicals. This channel requires the energy of 110.0/108.5(98.2/102.2) kcal/mol relative to HNCS(HSCN) which roughly corresponds to the experimental threshold energy (Table 3, Figure 6). The recombination of the two species would lead to both observed experimentally isomers, singlet HSCN and HSNC. Although this scenario fulfills the energy requirements, it does not reproduce the kinetics, since the singlet HSNC would be formed as a secondary product which is not the case according to the experimental data.

3.5.2. HNCS Isomerization on the Triplet PES. According to our calculations, the adiabatic excitation of the singlet HNCS precursor to its lowest triplet state (^{3}A) requires 67.1 kcal/mol. This value is still lower than the experimentally estimated threshold energy (300 nm, ca. 95 kcal/ mol).[10] Thus, the radiation used may lead to the triplet HNCS(^{3}A) molecules possessing an excess energy and resulting in the isomerizations. As can be seen from Figure 8, the most stable triplet species, branched-C(H)NS(^{3}A″), can be reached from HNCS(^{3}A) via TS1t(^{3}A) at the cost of 102 kcal/mol. However, a further isomerization to HSCN(^{3}A) via TS2t(^{3}A′) is highly endothermic and requires 126.1 kcal/mol, the activation energy with respect to branched-C(H)NS(^{3}A″) being 63.5 kcal/mol. The alternative and energetically more favorable channel leading to the triplet HSCN(^{3}A) begins with the dissociative step: branched-C(H)-NS(^{3}A″) → HCN + S(^{3}P). It involves a low-energy TS4t(^{3}A″) and leads to the HCN + S(^{3}P) dissociation products. This is followed by the HSCN(^{3}A) formation via TS5t(^{3}A″). The latter

Isomerization and Dissociation of CHNS

J. Phys. Chem. A, Vol. 107, No. 50, 2003 **11215**

TABLE 5: Comparison of the Predicted (Unscaled) and Observed IR Frequencies and Intensities (in Parentheses) for the Four Most Stable Singlet CHNS Isomers[a]

Isomer	Calculations		Experiment	Assignment	Symmetry
	B3LYP	MP2	Ar matrix[b]		
	3673 (245)	3710 (291)	3508.5 (0.33)	NH stretch	A'
	2040 (774)	2028 (724)	1981.8 (1.0)	CN stretch	A'
H—N—C—S	877 (3)	892 (2)	850.0 (0.01)	CS stretch	A'
	646 (337)	616 (377)	578.0 (0.20)	NCS bend	A'
	490 (3)	489 (8)		NCS bend	A''
	461 (78)	461 (93)		HNC bend	A'
	2656 (4)	2745 (9)	2581.0 (0.4)	SH stretch	A'
	2280 (21)	2129 (3)	2182.3 (1.0)	CN stretch	A'
H—S—C—N	978 (7)	979 (8)	959.7 (0.15)	HSC bend	A'
	693 (0)	708 (0)		CS stretch	A'
	404 (1)	379 (1)		SCN bend	A''
	339 (4)	329 (4)		SCN bend	A'
	3468 (357)	3480 (399)		CH stretch	A_1
	2138 (331)	1937 (651)		CN stretch	A_1
H—C—N—S	755 (53)	792 (88)		NS stretch	A_1
	428 (5)	426 (16)		CNS bend	E_1
	381 (58)	125 (49)		HCN bend	E_1
	2647 (0)	2745 (3)		SH stretch	A'
	2136 (133)	2064 (87)	2064.2	NC stretch	A'
H—S—N—C	1027 (10)	1040 (12)		HSN bend	A'
	689 (8)	707 (12)		SN stretch	A'
	287 (1)	280 (0)		SNC bend	A''
	225 (0)	230 (1)		SNC bend	A'

[a] Frequencies in cm^{-1}, calculated intensities in kmmol^{-1}, observed intensities relative to the most intense band. [b] Reference 10.

TABLE 6: Comparison of the Selected Energy Barriers (in kcal/mol) Calculated for Singlet CHNS and CHNO Isomerizations

reaction	energy barrier[a]		reaction	energy barrier	
	B3LYP//B3LYP	CCSD(T)//MP2		B3LYP//B3LYP[b]	G2[c]
HNCS → HSCN	62.4	60.3	HNCO → HOCN		88.0
HCNS → HSNC	59.8	58.2	HCNO → HONC		76.9
HSNC → cyclic-S(H)CN	19.2	18.3	HONC → cyclic-O(H)CN		25.0
HSCN → cyclic-S(H)CN	51.2	51.7	HOCN → cyclic-O(H)CN		85.9
HNCS → cyclic-N(H)CS	86.0		HNCO → cyclic-N(H)CO	123.7	120.2
cyclic-N(H)CS → HSCN	15.5		cyclic-N(H)CO → HOCN	33.6	34.0
HCNS → cyclic-C(H)NS	43.3		HCNO → cyclic-C(H)NO	69.8	73.2
HSNC → cyclic-C(H)NS	43.1		HONC → cyclic-C(H)NO	58.2	53.9

[a] This work. [b] Reference 25. [c] Reference 26.

transition state lies 100.7(33.7) kcal/mol above the singlet HNCS(HCN + S(^{3}P)) (Figure 9).

3.5.3. HNCS Isomerization on the Singlet PES. Let us assume that HNCS molecule being first excited by UV radiation decays from the excited PES to the ground state and the isomerization takes place on the singlet PES. As is apparent from section 3.2, starting from the singlet HNCS there are two paths available for the formation of singlet HSCN: one-step 1,3 hydrogen transfer via TS1 and the stepwise mechanism

involving TS5 and TS9. Starting from the same HNCS, there is no direct route for the formation of the second observed isomer singlet HSNC. However, as can be seen in Figures 4 and 5, the latter species can be produced as a secondary product from HSCN by the stepwise mechanism involving TS4 and TS3. Although the above routes might be accessible with the UV radiation used in the experiment,[10] this mechanism does not satisfy the kinetics requirements, since the singlet HSNC would not be formed as a primary product.

Further inspection of Figures 4 and 5 reveals that the only way to obey both energy and kinetics requirements is to take the singlet high-energy (59.3 kcal/mol) cyclic-S(H)CN isomer as a starting point on the ground PES for both isomerizations. According to the present calculations, the cyclic-S(H)CN is expected to be kinetically unstable and undergoes almost barrierless ring opening processes via TS3 and TS4 to form HSNC and HSCN species. The calculated barriers for these processes are 0.2/0.1 and 3.7/3.8 kcal/mol, respectively. Assuming such a mechanism all the experimental findings, including the fact that the third most stable isomer HCNS has not been observed, would be successfully explained. However, with the methods used in the present calculations, we are not able to establish the point where the excited HNCS decays to the ground state and initiates the HSCN and HSNC formation. Further computational work is clearly needed on the possible conical intersection mediating the HNCS photochemical reaction.[24]

3.6. Comparison with CHNO System, A systematic study of the potential energy surface governing the isomerization of the CHNO was carried out by Mebel et al.[25] and more recently by Shapley and Bacskay.[26] The CHNO isomers are well known oxygen analogues of the CHNS species. It seemed interesting to compare the singlet isomerization barriers presented in this paper for CHNS with those predicted for the CHNO (Table 6). Comparison of the results obtained for CHNO[25,26] with our CHNS results reveals the same ordering of the energy barriers for the corresponding isomerization processes. At the same time, the magnitude of the barriers involving the CHNS isomers is significantly smaller than those involving the CHNO counterparts.

4. Concluding Remarks

We have examined by quantum mechanical DFT B3LYP and ab initio MP2 and CCSD(T) methods the singlet and triplet potential energy surfaces for the isomerization and dissociation of CHNS. Our calculations have revealed nine singlet and eight triplet local minima. For singlet, isothiocyanic acid, HNCS, is the most stable isomer and global minimum followed by HSCN (11.8/6.3 kcal/mol higher in energy than HNCS), HCNS (34.3/34.4 kcal/mol), and HSNC (40.3/36.0 kcal/mol). For triplet, branched-C(H)NS(^{3}A″) species, which has no singlet analog, is the most stable isomer lying 62.6 kcal/mol above the global minumum. This is followed by the HNCS (^{3}A) isomer (67.1 kcal/mol).

Several possible routes for isomerization and dissociation have been identified on both PES's. The most stable singlet isomer HNCS can rearrange to HSCN via TS1 with the energy barrier of 62.4/60.3 kcal/mol. This can be compared with the HNCS → H + NCS dissociation energy of 89.0/89.6 kcal/mol. The activation energies for some isomerizations within the singlet CHNS system involving cyclic-N(H)CS (76.4/72.1 kcal/mol) and S(H)CN (59.3/54.2 kcal/mol) species are quite low (below 20 kcal/mol). In particular, the cyclic-S(H)CN undergoes almost barrierless (0.2/0.1 and 3.7/3.8 kcal/mol) ring-opening process via TS3 and TS4 to form HSNC and HSCN, respectively. The comparison shows that the singlet energy barriers calculated for the CHNS isomerizations are significantly smaller than those involving the CHNO counterparts.[25,26]

On the triplet PES, the most stable branched-C(H)NS(^{3}A″) (62.6 kcal/mol) isomer can easily dissociate to the HCN + S(^{3}P) products with the activation energy as low as 10 kcal/mol. This species can also rearrange to form HNCS(^{3}A) (67.1 kcal/mol) or HSCN(^{3}A) (90.1 kcal/mol) although with much higher activation energies of 39.9 and 63.5 kcal/mol, respectively.

On the basis of the presented results, an attempt has been undertaken to indicate a possible mechanism of the HNCS isomerization observed in the low-temperature matrixes.[10]

Judging from the previous DFT B3LYP studies on the related CHNO system[25,26] and the benchmark calculations of the species including the first and second row elements,[27] we expect our B3LYP/aug-cc-pVTZ energetics to be of reasonable accuracy. This is further supported by the comparison with the present CCSD(T)/aug-cc-pVTZ energetics. However, the latter also reveals some differences in the predictions of the two methods, most significantly for the dissociation energies. In this respect, our conclusion is consistent with that of Shapley and Bacskay for CHNO.[26]

References and Notes

(1) Yamada, K.; Winnewisser, M.; Winnewisser, G.; Szalanski, L. B.; Gerry, M. C. L. *J. Mol. Spectrosc.* **1979**, *78*, 189.

(2) Yamada, K.; Winnewisser, M.; Winnewisser, G.; Szalanski, L. B.; Gerry, M. C. L. *J. Mol. Spectrosc.* **1980**, *79*, 295.

(3) Durig, J. R.; Wertz, D. W. *J. Chem. Phys.* **1967**, *16*, 3069.

(4) Draper, G. R.; Werner, R. L. *J. Mol. Spectrosc.* **1974**, *50*, 369.

(5) Wierzejewska, M.; Wieczorek, R. *Chem. Phys.* **2003**, *287*, 169.

(6) Wierzejewska, M.; Olbert-Majkut, A. *J. Phys. Chem. A* **2003**, *107*, 1928.

(7) McDonald, J. R.; Scherr, U. M.; McGlynn, S. P. *J. Chem. Phys.* **1969**, *51*, 1723.

(8) Boxall, C. R.; Simons, J. P. *J. Photochem.* **1972−74**, *1−2*, 363.

(9) Ruscic, B.; Berkowitz, J. *J. Chem. Phys.* **1994**, *101*, 7975.

(10) Wierzejewska, M.; Mielke, Z. *Chem. Phys. Lett.* **2001**, *349*, 227.

(11) Dunning, T. H. *J. Chem. Phys.* **1989**, *90*, 1007.

(12) Kendall. R. A.; Dunning, T. H.; Harrison, R. J. *J. Chem. Phys.* **1992**, *96*, 6796.

(13) Woon, D. E.; Dunning, T. H. *J. Chem. Phys.* **1993**, *98*, 1358.

(14) Becke, A. D. *J. Chem. Phys.* **1993**, *98*, 5648.

(15) Lee, C.; Yang, W.; Parr, R. G. *Phys. Rev. B* **1988**, *37*, 785.

(16) Gonzalez, C.; Schlegel, H. B. *J. Chem. Phys.* **1989**, *90*, 2154.

(17) Gonzalez, C.; Schlegel, H. B. *J. Chem. Phys.* **1990**, *94*, 5523.

(18) Pople, J. A.; Binkley, J. S.; Seeger, R. *Int. J. Quantum Chem. Symp.* **1976**, *10*, 1.

(19) Raghavachari, K.; Trucks, G. W.; Pople, J. A.; Head-Gordon, M. *Chem. Phys. Lett.* **1989**,*157*, 479.

(20) Frish, M. J.; Trucks, G. W.; Schlegel, H. B.; Scuseria, G. E.; Robb, M. A.; Cheesman, J. R.; Zakrzewski, V. G.;. Montgomery, J. A., Jr; Stratmann, R. E.; Burant, J. C.; Dapprich, S.; Millam, J. M.; Daniels, A. D.; Kudin, K. N.; Strain, M.; Farkas, O.; Tomasi, J.; Barone, V.; Cossi, M.; Cammi, R.; Mennucci, B.; Pomelli, C.; Adamo, C.; Clifford, S.; Ochterski, J.; Petersson, G. A.; Ayala, P. Y.; Cui, Q.; Morokuma, K.; Malick, D. K.; Rabuck, A. D.; Raghavachari, K.; Foresman, J. B.; Cioslowski, J.; Otriz, J. V.; Baboul, A. G.; Stefanov, B. B.; Liu, G.; Liashenko, A.; Piskorz, P.; Komaromi, I.; Gomperts, M.; Martin, R. L.; Fox, D. J.; Keith, T.; Al.-Laham, M. A.; Peng, C. Y.; Nanayakkara, A.; Challacombe, M.; Gill, P. M. W.; Johnson, B.; Chen, W.; Wong, M. M.; Andres, J. L.; Gonzales, C.; Head-Gordon, M.; Replogle, E. S.; Pople, J. A. *Gaussian 98,* Revision A.9; Gaussian Inc.: Pittsburgh, PA, 1998.

(21) Bak, B.; Christiansen, J. J.; Nielsen, O. J.; Svanholt, H. *Acta Chim. Scand. A* **1977**, *31*, 666.

(22) Leung, H.; Suffolk, R. J.; Watts, J. D. *Chem. Phys.* **1986**, *109*, 289.

(23) Gerbaux, P.; Van Haverbeke, Y.; Flammang, R.; Wong, M. W.; Wentrup, C. *J. Phys. Chem. A* **1997**, *101*, 6970.

(24) Olivucci, M. *Chim. Ind.* **2002**, *84* (7), 1 and references therein.

(25) Mebel, A. M.; Luna, A.; Lin, M. C.; Morokuma K. *J. Chem. Phys.* **1996**, *105*, 6439.

(26) Shapley, W. A.; Bacskay, G. B. *J. Phys. Chem. A* **1999**, *103*, 6624.

(27) Bauschlicher, C. W.; Patridge, H. *Chem. Phys. Lett.* **1995**, *240*, 533.

(28) Northrup, F. J.; Sears, T. J. *J. Chem. Phys.* **1990**, *93*, 2346.